Random Multiple Scattering Enhanced Photoacoustic Gas Spectroscopy with Disordered Porous Ceramics

Haihong Bao[a,b], Congzhe Zhang[a,b], Yinping Miao[a,b*] and Wei Jin[a,b*]

[a]Department of Electrical Engineering, The Hong Kong Polytechnic University, Hung Hom, Kowloon, Hong Kong, China;

[b] Photonic Sensors Research Center, The Hong Kong Polytechnic University Shenzhen Research Institute, Shenzhen, 518057, China

ABSTRACT: Light-gas interaction can be enhanced by using disordered porous materials since multiple random scattering increases light intensity near the surface of the material. Here we report signal enhancement of photoacoustic gas spectroscopy with disordered porous ceramics. The amplitude and frequency characteristics of photoacoustic signal due to gas absorption in disordered materials are modeled theoretically. Experiment with a porous Al_2O_3 sample demonstrates photoacoustic signal enhancement of ~ 4 times at 5 kHz.

KEYWORDS: *photoacoustic signal enhancement, gas spectroscopy, porous material, light localization, random multiple scattering, optical fiber sensor.*

INTRODUCTION

Photoacoustic spectroscopy(PAS) is a powerful technique for trace chemical molecules and has been widely used in various fields of physics, chemistry and biology[1]. Photoacoustic (PA) signals are generated from light absorption of targeted molecules, resulting in local heating and generation of acoustic pressure waves. With narrow-band laser sources and sensitive acoustic detection devices, highly sensitive PAS gas sensors with good selectivity have been demonstrated[2–4]. In PAS gas sensors, the PA signal is proportional to light energy absorbed by the gas molecules. Light absorption is described by the Beer-Lambert law: $\Delta I=I_0(1-e^{-\mu_a L})$, where I_0 is the incident light intensity, μ_a is the absorption coefficient and L is the absorption path length. Larger the values of μ_a and L, stronger absorption and hence stronger the PA signal. However, the value of L is limited by the detection area of the acoustic detectors. Stronger PA signals may be obtained with multi-pass optical cavities to enhance laser power that interacts with the gas molecules. With a high finesse optical cavity, demonstration of optical power build up by a factor of 1000 has been demonstrated[5]. Higher power buildup may be achieved by employing an intra-cavity configuration[6]. However, it is difficult to implement a stable optical cavity with high finesse, and extra electronic feedback and complicated alignment process are typically needed for stable operation of the cavity.

Light absorption can be enhanced in a highly disordered material[7]. As shown in Figure 1, each time a scattering event occurs, the light propagation direction is forced to change, and most transmitted photons have gone through a longer path length compared to the sample thickness. The number of photons directly transmitted through the sample is quite small and the Beer-Lambert law alone is found inadequate to describe photon distribution if scattering effect is taken into consideration. Quantitative models describing photon distribution have been established by using diffusion theory[8,9]. It is found that photon distribution is shifted toward the sample surface, increasing localized light intensity due to multiple scattering[1,10].

Here we propose utilizing the light localization resulting from random multiple scattering to enhance PA signal of trace gas embedded in solid porous materials. This new PA enhancement mechanism has the potential to improve the performance of PAS gas sensors while require neither accurate alignment nor extra optical stabilization.

THEORY

1. Light Intensity Distribution

The physical process and quantitative description of photon migration in disordered samples have been well investigated. For disordered samples satisfying Ioffe–Regel criterion $kl\leq1$ where $k=2\pi/\lambda$ *i*s the light wave number and l is the transport mean free path, interference induced light localization is expected to occur. However, most disordered materials have the value $kl\gg1$ where wave interference can be neglected and and the photon behavior can be described by radiative transfer equation (RTE)[11–14]. The time dependent RTE describing the energy flux moving in direction $\hat{s}$ is defined as[15,16]:

$$\frac{1}{v}\frac{\partial L(r,t,\hat{s})}{\partial t}+\hat{s}\cdot\nabla L(r,t,\hat{s})$$
$$=-\mu_t L(r,t,\hat{s})+\frac{\mu_s}{4\pi}\int_{4\pi}p(\hat{s},\hat{s}')L(r,t,\hat{s})d\omega'+S(r,t,\hat{s})$$

(1)

where v isthe average light velocity inside scattering sample; $L(r,t,\hat{s})$ is radiance in $Wsr^{-1}m^{-2}$; $\mu_t=\mu_a+\mu_s$ is the extinction coefficient with scattering coefficient μ_s and absorption coefficient μ_a; $p(\hat{s},\hat{s}')$ is the probability of photons scattered from direction $\hat{s}$ into $\hat{s}'$ and $S(r,t,\hat{s})$ is the source term.

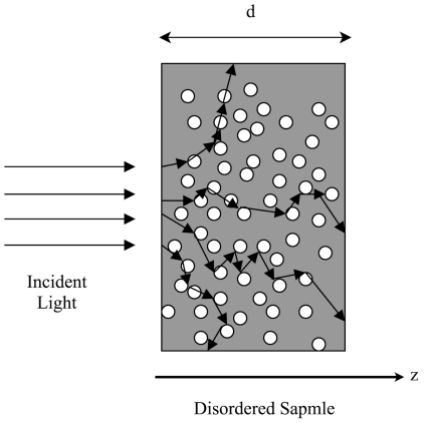

Figure 1. Light scattering in disordered material.

Considering a continuous wave (CW) propagating in a disordered sample in a slab geometry of thickness d with z = 0 at the illuminated air-sample boundary, as shown in Figure 1, the steady state photon number at surface z may be obtained from Equation (1) and denoted as[16]:

$$L(z)=-2D\frac{\partial[F_+(z)+F_-(z)]}{\partial z}+D\mu_t L_0\exp(-\mu_t z)$$

(2)

where $D=1/(3*\mu_s)$ for isotropic scattering; $F_\pm(z)$ is the forward/backward flux going through a small area of the surface within the sample and it is determined by μ_a and μ_s of disordered sample. L_0 is the isotropic source term. The explicit form of $F_\pm(z)$ can be found in reference[17].

For samples with large absorption, most photons are absorbed before scattering occurs. Hence, we only consider weak absorption case here, in which case $1/\mu_a$ is much larger than sample thickness d. For disordered material with small absorption coefficient, the scattering may be regarded as isotropic; the calculated light intensity distributions along the propagation direction z for different scattering coefficients are shown in Figure 2. The penetration length into the sample is significantly modified at presence of strong scattering and the photon density shifts towards the surface region as the scattering coefficient increases. The change of photon density distribution results from the fact that each time scattering occurs, many photons are backward scattered resulting higher light intensity being localized near the surface of the sample.

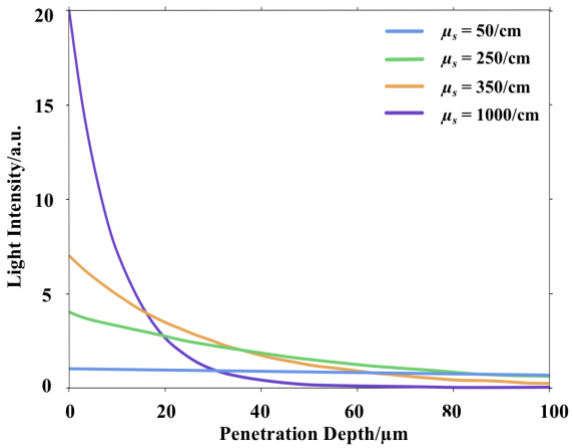

Figure 2. Light intensity distribution in a porous material.

2. PA Signal Generation

When the pump laser wavelength is tuned to the absorption center of gas molecules, the molecules are heated up generating PA signal. Here, we focus on frequency dependent PA signal and its dependence on material parameters, i.e., scattering coefficient and pore size. Assuming perfect energy conversion from absorbed light to heat, the heat generated within {z, z+dz} in the sample would be:

$$[\varepsilon\mu_{a\_gas}+(1-\varepsilon)\mu_{a\_solid}]L(z)dz$$

(3)

where $\varepsilon=V_{gas}/(V_{gas}+V_{solid})$ is the sample porosity defined by the volume ratio of the embedded gas. μ_{a_gas} and μ_{a_solid} are the absorption coefficient of the embedded gas and solid porous material respectively. Both embedded gas and solid material of the disordered sample will absorb light and generate heat. The acoustic signal results from the heated interstitial gas expansion and thermal conduction from the heated solid sample to surrounding gas and its expansion[18]. However, solid material usually has much wider absorption spectra than gases. When the wavelength of the pump laser is scanned over the gas absorption line, the PA signal generated from solid material absorption only contributes to a flat background signal. Thus, the PA signal due to gas absorption can be expressed as $\varepsilon\mu_{a\_gas}L(z)dz$. In addition, pore-size dependent pressure wave attenuation would modify the detected PA signal.

For air, the viscous penetration depth d_f is evaluated as $2.2*10^3/\sqrt{f}$ (μm) at acoustic frequency f, and $d_f \approx 13.9$ μm for f = 25 kHz[18]. Now considering a simplified model that the porous sample consists of a bunch of cylindrical tubes whose diameter equals to the porosity diameter 2R. If 2R<d_f, the acoustic pressure wave would attenuate in an exponent way as $\exp(-z/l_{ac})$; where $l_{ac} \approx 7*10^3*2R/\sqrt{f}$ (μm) [18]. The PA signal detected at the surface where pump light is incident into porous material may be expressed as:

$$\mu_{a\_gas} \int_0^d I(z)\exp(-z/l_{ac})dz \qquad (4)$$

From equation (4), it is obvious that the PA signal is strongly depended on the sample porosity, gas absorption and acoustic attenuation property of the sample. A sample with smaller pore size would generate smaller PA signal due to larger acoustic attenuation (smaller l_{ac}). For constant light laser power, the PA signal as function of laser modulation frequency, i.e., the generated acoustic frequency, were calculated for samples with different pore sizes and are shown in Figure 3. In the calculation, we have used porosity: 50%, sample length: 1cm, μ_{a_gas} = μ_{a_solid}=0.01 cm^{-1} and μ_s= 300 cm^{-1}, which are close to the experimentally measured values of our samples and satisfy the weak absorption condition.

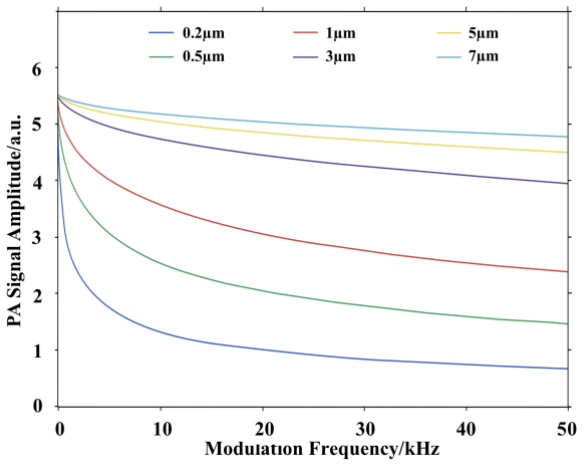

Figure 3. Calculated PA signal amplitude versus laser modulation frequency for different pore sizes. The radius of pores ranging from 0.2 to 7 μm are used for calculation.

The PA signals at surface z=0 were also calculated for different scattering coefficients and are depicted in Figure 4. The sample parameters used in calculation are porosity: 50%, sample length: 1cm, μ_{a_gas} = μ_{a_solid} = 0.01cm^{-1} and the pump light modulation frequency is 25 kHz. Stronger PA signal is expected with higher scattering coefficient and larger pore size when other detecting conditions kept unchanged.

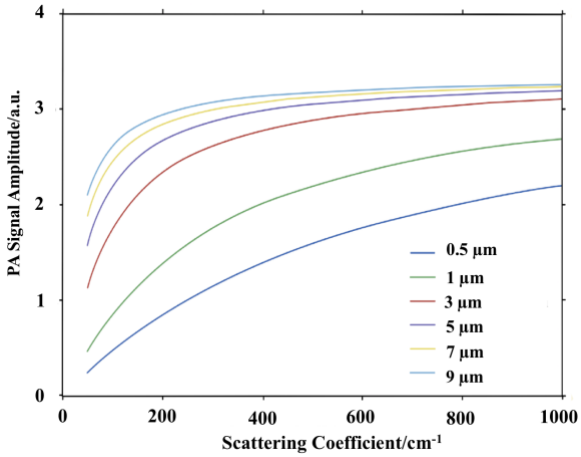

Figure 4. Calculated PA signal amplitude versus scattering coefficient for different pore sizes at 25kHz. The radius of pores ranging from 0.5 to 9 μm are used for calculation.

EXPERIMENT

1. Determination of μ_a and μ_s of the Disordered Sample

As discussed in the former section, the absorption and scattering characteristics of the disordered sample have significant impact on the photon distribution. The absorption coefficient and scattering coefficient can be actually evaluated by nonlinear fitting the time-of-flight (TOF) curve using a short pulse laser[19]. An equivalent way to determine the TOF curve is using frequency modulation continuous wave (FMCW) interferometry technique[20].

The experiment setup of FMCW interferometry is depicted in Figure 5 (a). The light source is an external cavity laser (ECDL) (Agilent, 81600B) whose wavelength is linearly swept around 1540 nm with a triangular waveform. The output light is divided into two beams by 10:90 coupler (coupler 1). The signal beam experiences multiple scattering when going through the disordered sample. Then reference beam interferes with the signal beam light at a 50:50 coupler (coupler 2). The disordered samples used here are porous Al_2O_3 ceramics with average pore size of ~5 μm and ~10 μm (YongGuang Chemical Packing Co., Ltd). The thicknesses of these samples are 3.91 mm and 3.03 mm, respectively. The porosity is ~40%.

If there is no porous sample placed between the collimator pair, the optical path difference (OPD) between the signal beam and reference beam induces a single beating frequency signal. The beat frequency Δf is well defined and is proportional to the time delay difference τ between the two arms, as illustrated in

Figure 5(b). The frequency spectrum of this beat signal is depicted as the green line in Figure 6. When a porous material is placed between the collimator pair, the random multiple scattering creates a distribution of extra optical OPD or time delay, which leads to the broadening of the beating frequency range. Stronger scattering process leads to larger mean value and wider line width of the detected beating frequency signal[21]. For two porous Al_2O_3 ceramics with pore size of diameter of ~5 µm and ~10 µm, the power spectra of the detector output are shown in Figure 6 as the blue and red curves respectively. μ_a and μ_s of the sample can be retrieved by nonlinear fitting which minimizes the squared norm of the difference between the time delay curve derived from RTE and that measured by experiment[22]. It was determined that the scattering coefficient μ_s of the two porous Al_2O_3 ceramics used in experiment are 353.73 cm^{-1} and 193.45 cm^{-1}, respectively. The absorption coefficients μ_a for those ceramic samples are 0.023 cm^{-1} and 0.16 cm^{-1}, which are negligible compared with $1/d$ satisfying weak absorption condition.

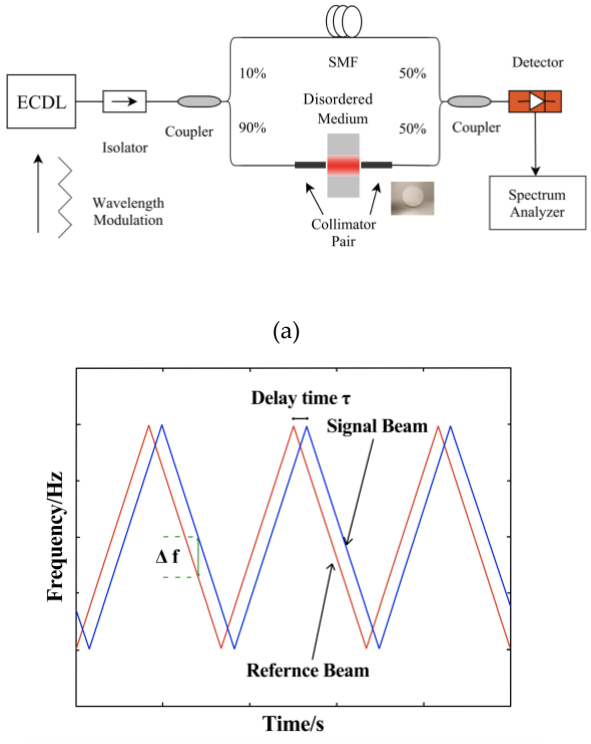

Figure 5. (a) Experimental setup of the FMCW heterodyne detection system. (b) Principle of FMCW

2. Validation of PA Signal Enhancement

To validate the PA signal enhancement due to the multiple scattering, a PAS detection system is built as shown in Figure 7. Light from a distributed feedback laser (DFB) diode is amplified by an erbium-doped amplifier (EDFA) and used as the pump light source. Passing through the tunable filter which filters out the amplified spontaneous emission (ASE) noise, the pump light is incident on the disordered sample. The pump light is wavelength modulated at frequency 5 kHz while its wavelength is slowly tuned across the P(9) absorption line of acetylene at 1530.371 nm. The pump light delivered in the gas cell is estimated to be ~25mW and the beam diameter is about ~0.5mm. The gas absorption-induced PA signal is detected by a fiber-tip microphone made of graphene film and is placed near the surface of the disordered material. The fiber-tip microphone is demodulated by a Sagnac interferometer with a 3*3 loop coupler. Detailed description of the fiber-tip microphone and the demodulation system can be found in references[23,24]. The gas sample is 7500 ppm acetylene balanced in nitrogen and the porous sample is 3.93 mm thick with ~5 μm diameter as tested in former section.

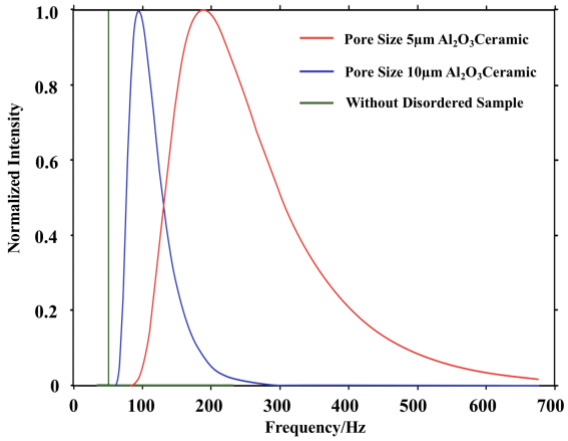

Figure 6. Power spectra of detected light signal going through different porous ceramics

Figure 8 shows the measured second harmonic output from the lock-in amplifier when the pump laser wavelength is scanned across the P(9) absorption line of acetylene. The signals with and without the use of the disordered medium are shown as green and blue curves respectively. Compared with the conventional free-space PA system, the PA signal is enhanced ~4 times with the presence of scattering sample when pump laser is modulated at 5 kHz.

The enhanced PA signal with the use of scattering sample may be considered resulting from contributions of two different physical origins: acoustic signal generated from light absorption by gas molecules and by solid material of porous sample. The detected PA responses of acetylene gas and solid porous material are shown respectively as the red and blue lines in Figure 9. The PA responses of acetylene was detected without the

disordered sample located in the system while the PA signal generated from the solid material is obtained without the presence of acetylene gas. It is found out that the PA signal generated from gas absorption has a Lorentzian shape while that generated from solid material absorption is nearly flat as pump light wavelength was scanned over the gas absorption line. The amplitude of the PA signal due to solid material absorption is much smaller than that due to gas absorption. Hence, the PA signal generated from the expansion of interstitial gas volume dominates the detected signal of the porous sample shown in Figure 8.

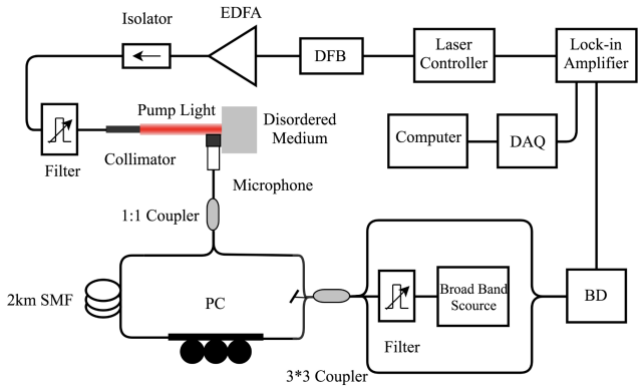

Figure 7. Experimental setup of PAS gas detection system. BD: Balanced detector; PC: Polarization controller; SMF: Single mode fiber.

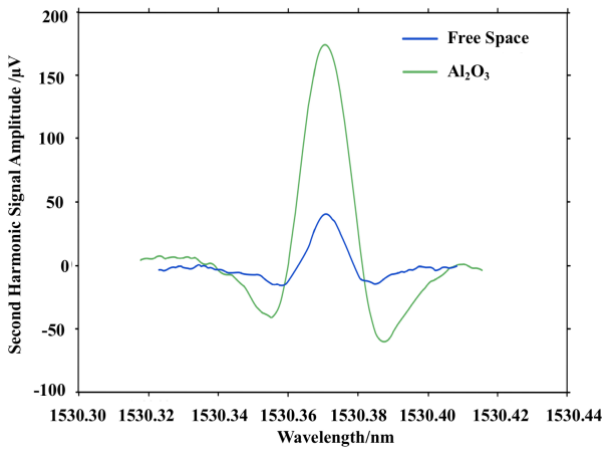

Figure 8. Second harmonic lock-in output with and without the presence of porous ceramics. The laser modulation frequency is 5 kHz.

The signal at the lock-in output was found depending strongly on the modulation frequency of the pump laser, because of the following reasons: firstly, as indicated in Figure 3, higher frequency PA signal is expected to experience stronger attenuation in the porous material and hence the PA signal generated at the microphone is smaller for high acoustic frequency. Secondly, the transfer functions of the microphone and the Sagnac demodulation system are also frequency dependent. The signal at the output of the Sagnac interferometer may be expressed as $S(f)M(f)\sin(\rho Lf/v)$, where $S(f)$ is the generated PA signal, $M(f)$ is frequency response of microphone, $\sin(\rho Lf/v)$ is the transfer function of the Sagnac interferometer. v is light speed in single mode fiber, f is laser modulation frequency and L is length of the fiber delay line. As a result, the frequency response of generated PA signal can be extracted from the demodulated signal $S_A(f)/S_F$ where $S_A(f)$ and S_F are the generated PA signal with and without Al_2O_3 porous ceramics respectively. The extracted signal then is normalized and shown in Figure 10. Resonant frequency of graphene film is avoided intentionally to detect faithful frequency response of acoustic signal[23,24]. It is shown that at low frequency region (less than 10 kHz), PA signal increases dramatically as laser modulation frequency drops which indicates that acoustic signal is attenuated quickly with increasing frequency in low frequency region (<10 kHz). Above 10 kHz, similar to thermally induced ultrasonic emission from porous silicon[25], the PA emission is flat over a wider frequency range (from 10 to 40 kHz). The detected result generally agrees well with frequency response trend predicted in Figure 2. Even though PA signals experiences attenuation within disordered sample, the detected PA signal is still ~1.5 times PA signal detected in free space. There is no contribution of acoustic resonance to the amplified PA signal due to the disordered nature of the porous sample. It might be possible to design porous structures that have acoustic resonances, and the combination of the random light scattering enhancement and acoustic resonant enhancement would further enhance the detected PA signal. It should be pointed out that, though both theory and experiment results indicate that larger PA may be generated at lower modulation frequency, larger environment noise sources (acoustic noise, vibrations, etc.) are located at low frequency region, which would notably deteriorate the signal to noise ratio (SNR).

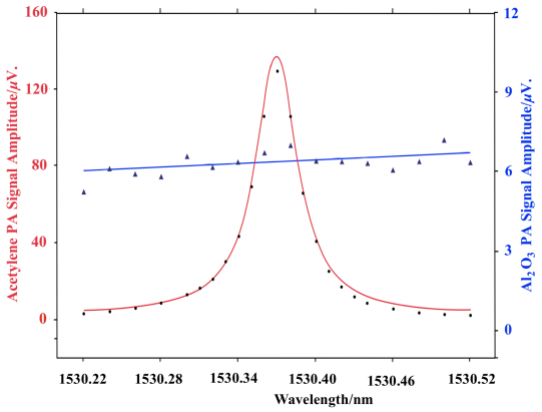

Figure 9. Detected PA response of acetylene and Al_2O_3 porous ceramics. The dots are the measured data and the lines are the fitting results. The measured PA signal generated from gas absorption is fitted to the Lorentz line shape.

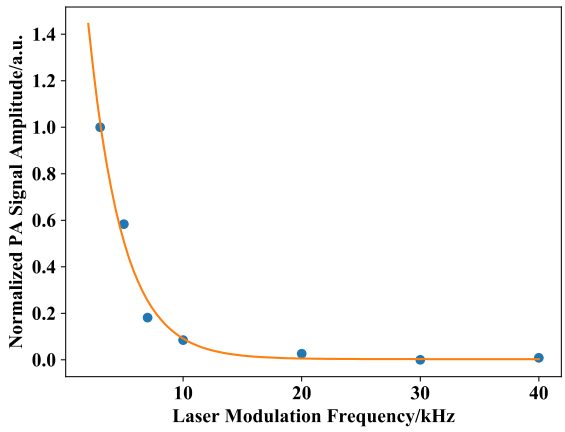

Figure 10. Extracted frequency response of generated PA signal with presence of porous ceramic.

CONCLUSIONS

It is concluded that PA signal can be enhanced by random multiple scattering within porous samples. Theoretical modelling shows that stronger PA signal can be generated with porous materials with larger scattering coefficients and operating at lower laser modulation frequency. A simple PA gas detection experiment with commercial Al_2O_3 porous ceramics demonstrated an enhancement factor of ~4 at 5 kHz over the conventional PA system. At higher frequencies from 10 to 40 kHz, the PA signal is almost independent of the acoustic frequency with an enhancement factor of ~ 1.5. The principle of PA signal enhancement is valid for other porous material and the larger enhancement could be achieved by optimizing the parameters of the porous material. Based on a similar principle, it is also possible to demonstrate laser-controlled ultrasound generation and the magnitude of PA signal could be further enhanced by using mid-infrared pump lasers where gas molecules have much stronger absorption.

AUTHOR INFORMATION

Corresponding Author

* Email: kikosi@126.com (Yinping Miao)
* Email: wei.jin@polyu.edu.hk (Wei Jin)

Funding Sources

This work was supported in part by the Hong Kong SAR government under GRF Grant PolyU 152229/15E, in part by the Natural Science Foundation of China under NSFC Grants 61535004, and in part by the Hong Kong Polytechnic University under Grants 4BCD1 and 1ZVG4.

REFERENCES

(1) Tam, A. C. Appliacations of Photoacoustic Sensing Techniques. Rev. Mod. Phys. **1986**, 58 (2), 381–431.

(2) Pietro Patimisco, Angelo Sampaolo, Lei Dong, Frank K. Tittel, and V. S. Recent Advances in Quartz Enhanced Photoacoustic Sensing. Appl. Phys. Rev. **2018**, 5 (1), 011106.

(3) Wu, H.; Dong, L.; Zheng, H.; Yu, Y.; Ma, W.; Zhang, L.; Yin, W.; Xiao, L.; Jia, S.; Tittel, F. K. Beat Frequency Quartz-Enhanced Photoacoustic Spectroscopy for Fast and Calibration-Free Continuous Trace-Gas Monitoring. Nat. Commun. **2017**, 8, 1–8.

(4) Zheng, H.; Dong, L.; Wu, H.; Yin, X.; Xiao, L.; Jia, S.; Curl, R. F.; Tittel, F. K. Application of Acoustic Micro-Resonators in Quartz-Enhanced Photoacoustic Spectroscopy for Trace Gas Analysis. Chem. Phys. Lett. **2018**, 691, 462–472.

(5) Hippler, M.; Mohr, C.; Keen, K. A.; McNaghten, E. D. Cavity-Enhanced Resonant Photoacoustic Spectroscopy with Optical Feedback CW Diode Lasers: A Novel Technique for Ultratrace Gas Analysis and High-Resolution Spectroscopy. J. Chem. Phys. **2010**, 133 (4), 044308.

(6) Starovoitov, V. S.; Kischkat, J. F.; Semtsiv, M. P.; Ted Masselink, W. Intracavity Photoacoustic Sensing of Water Vapor with a Continuously Tunable External-Cavity Quantum-Cascade Laser Operating near 55 Mm. Opt. Lett. **2016**, 41 (21), 4955.

(7) Svensson, T.; Adolfsson, E.; Lewander, M.; Xu, C. T.; Svanberg, S. Disordered, Strongly Scattering Porous Materials as Miniature Multipass Gas Cells. Phys. Rev. Lett. **2011**, 107 (14), 1–4.

(8) Martelli, F.; Bassani, M.; Alianelli, L.; Zangheri, L. Accuracy of the Diffusion Equation to Describe Photon Migration through an Infinite Medium: Numerical and Experimental Investigation. Phys. Med. Biol. **2000**, 1359.

(9) Yasa, Z. a; Jackson, W. B.; Amer, N. M. Photothermal Spectroscopy of Scattering Media. Appl. Opt. **1982**, 21 (I), 21–31.

(10) Helander, P.; Lundström, I.; McQueen, D. Light Scattering Effects in Photoacoustic Spectroscopy. J. Appl. Phys. **1980**, 51 (7), 3841–3847.

(11) Garcia, N.; Genack, A. Z.; Lisyansky, A. A. Measurement of the Transport Mean Free Path of Diffusing Photons. Phys. Rev. B **1992**, 46 (22), 14475–14479.

(12) Pierrat, R.; Ambichl, P.; Gigan, S.; Haber, A.; Carminati, R.; Rotter, S. Invariance Property of Wave Scattering through Disordered Media. Proc. Natl. Acad. Sci. **2014**, 111 (50), 17765–17770.

(13) Wiersma, D. S.; Bartolini, P.; Lagendijk, A.; Righini, R. Localizationof Light Ina Disorderedmedium. Nature **1997**, 390 (6661), 671–673.
(14) Wiersma, D. S. The Physics and Applications of Random Lasers. Nat. Phys. **2008**, 4 (5), 359–367.
(15) Haskell, R. C.; Svaasand, L. O.; Tsay, T. T.; Feng, T. C.; McAdams, M. S.; Tromberg, B. J. Boundary Conditions for the Diffusion Equation in Radiative Transfer. J. Opt. Soc. Am. A Opt. image Sci. **1994**, 11 (10), 2727–2741.
(16) Contini, D.; Martelli, F.; Zaccanti, G. Photon Migration through a Turbid Slab Described by a Model Based on Diffusion Approximation I Theory. Appl. Opt. **1997**, 36 (19), 4587.
(17) Welch, A. J.; Van Gemert, M. J. C. Optical-Thermal Response of Laser-Irradiated Tissue; **2011**.
(18) Bernini, U.; Maddalena, P.; Massera, E.; Ramaglia, A. Photo-Acoustic Characterization of Porous Silicon Samples. J. Opt. A Pure Appl. Opt. **1999**, 1 (2), 210–214.
(19) Mei, L.; Lundin, P.; Andersson-Engels, S.; Svanberg, S.; Somesfalean, G. Characterization and Validation of the Frequency-Modulated Continuous-Wave Technique for Assessment of Photon Migration in Solid Scattering Media. Appl. Phys. B Lasers Opt. **2012**, 109 (3), 467–475.
(20) Guan, Z.; Lundin, P.; Svanberg, S. Assessment of Photon Migration in Scattering Media Using Heterodyning Techniques with a Frequency Modulated Diode Laser. Opt. Express **2009**, 17 (18), 16291.
(21) Mei, L.; Somesfalean, G.; Svanberg, S. Frequency-Modulated Light Scattering Interferometry Employed for Optical Properties and Dynamics Studies of Turbid Media. Biomed. Opt. Express **2014**, 5 (8), 2810.
(22) Borycki, D.; Kholiqov, O.; Chong, S. P.; Srinivasan, V. J. Interferometric Near-Infrared Spectroscopy (INIRS) for Determination of Optical and Dynamical Properties of Turbid Media. Opt. Express **2016**, 24 (1), 329.
(23) Ma, J.; Yu, Y.; Jin, W. Demodulation of Diaphragm Based Acoustic Sensor Using Sagnac Interferometer with Stable Phase Bias. Opt. Express **2015**, 23 (22), 29268.
(24) Ma, J.; Xuan, H.; Ho, H. L.; Jin, W.; Yang, Y.; Fan, S. Fiber-Optic Fabry-Pérot Acoustic Sensor with Multilayer Graphene Diaphragm. IEEE Photonics Technol. Lett. **2013**, 25 (10), 932–935.
(25) Shinoda, H.; Nakajima, T.; Ueno, K.; Koshida, N. Thermally Induced Ultrasonic Emission from Porous Silicon. Nature **1999**, 400 (6747), 853–855.

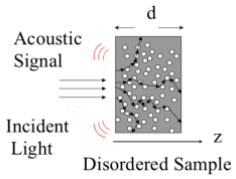
d
Acoustic
Signal
Incident
Light
z
Disordered Sample